Available online at www.sciencedirect.com
ScienceDirect
Geochimica et Cosmochimica Acta 73 (2009) 5320–5332
Geochimica et Cosmochimica Acta
www.elsevier.com/locate/gca

Oxygen isotopic signature of the skeletal microstructures in cultured corals: Identification of vital effects

A. Juillet-Leclerc [a,*], S. Reynaud [b], C. Rollion-Bard [c], J.P. Cuif [d], Y. Dauphin [d], D. Blamart [a], C. Ferrier-Pagès [b], D. Allemand [b]

[a] LSCE Domaine du CNRS, 91198 Gif sur Yvette, France
[b] CSM Avenue Saint-Martin, MC-98000 Monaco, Principality of Monaco, France
[c] CRPG-CNRS, Nancy-Université, B.P. 20, 54 501 Vandoeuvre-lès-Nancy Cedex, France
[d] UMR IDES 8148 du CNRS, Université Paris XI, 91405 Orsay, France

Received 19 May 2008; accepted in revised form 27 May 2009; available online 14 June 2009

Abstract

In order to identify vital effect on oxygen isotopic ratio, we analyzed at micrometer size scale skeleton microstructures of a scleractinian coral *Acropora*, cultured under constant conditions. Measurements focused on the two crystalline units highlighted different isotopic signatures. Massive crystals (centers of calcification: COC) exhibit quasi-constant lowest values whereas fibers, the dominant units exhibit scattered distribution with amplitude of up to 5‰. Fiber oxygen isotopic ratios ($\delta^{18}O$) range from values similar to instantaneous deposition to equilibrium value. By comparing data obtained on the *Acropora* specimen and deep-sea corals grown under well constrained conditions, we infer that the scattered $\delta^{18}O$ aragonite fibers indicate precipitation through kinetic precipitation. Thus, we argue for inherent biological feature typical to all coral genera. Modalities of COC formation remain ignored.

The different isotopic signature of two mineral microstructures present in close proximity in coral skeleton can only be explained by compartment depositions related to different organic environments. Indeed, multiple secondary electron microscopy (SEM) observations favor interaction between mineral and organic matrix surface. Moreover, atomic forcing microscopy (AFM) investigations demonstrated thermodynamic changes induced by mineralization in presence of organic compounds. The combination of our results with previous published ones from biological studies, allows us proposing a consistent model of fiber skeleton formation. The prerequisite step of mineral growth unit precipitation would be initiated by organic matrix secretion, which defines spatial extension. Specific carriers supply ionic compounds of the crystals to ensure local supersaturation. However, possibly controlled by organic molecules, ionic amount would be limited, implying the supersaturation decline over the time. This could explain the progressive decrease of the coral growth rate. In this case, vital effect should not only bias isotopic fractionation through biological activity but the mechanism of skeleton deposition is imposed by specific chemical and/or physical conditions due to the presence of organic molecules. These conclusions derive from observations performed at high resolution.

Therefore, isotopic ratio measured on millimeter scale for paleoclimatic purposes, result of the average of strongly heterogeneous values. It could explain vital effects shown by geochemical time series derived from tropical coral skeleton, including the high species and/or colony variability.

1. INTRODUCTION

The ability of coral skeletons to record environmental variability has been investigated by many authors during the last two decades (McConnaughey, 1989a; Cole et al.,

* Corresponding author. Address: LSCE Domaine du CNRS, Avenue de la Terrasse, 91198 Gif sur Yvette, France.
E-mail address: Anne.Juillet-Leclerc@lsce.ipsl.fr (A. Juillet-Leclerc).

0016-7037/$ - see front matter © 2009 Elsevier Ltd. All rights reserved.
doi:10.1016/j.gca.2009.05.068

1993; Dunbar et al., 1994; Wellington et al., 1996). However, the geochemistry of the coral skeleton, like most other biogenic minerals, is influenced both by environment (temperature, light, salinity, etc) and by biological activity (respiration, feeding, spawning, calcification) (Weiner and Dove, 2003), often referred to as "vital effect" (Urey et al., 1951). Vital effect could also include photosynthesis (Reynaud-Vaganay et al., 2001; Grottoli, 2002) as some corals live in symbiosis with algae (zooxanthellae). Analyses carried out at millimeter scale have improved our understanding of the geochemistry of the coral skeleton, but they did not take into account its microstructure, which is more complex than previously thought.

From a microstructural viewpoint, coral skeletons are composed of two main components, the centers of calcification (COC) and fibers. Ogilvie (1896) was the first to describe COC as the points from which fibers diverge. Then Le Tissier (1988) and Hidaka (1991) identified structural differences between fibers and COC. More recently, it was shown that COC and fibers did differ in size and shape, and also in their associated biochemical environment (Cuif et al., 2003).

Rollion-Bard et al. (2003a) performed the first micrometer-scale isotopic analyses using ion microprobe on *Porites lutea*. Though isotopic data seemed to be distributed according to morphology, unfortunately, the authors could not characterize isotopic data of individual crystal unit in *Porites*, due to the small size of the microstructures (less than 10 μm) compared with the spot size of ion microprobe (between 30 and 50 μm). In contrast, with larger crystal units, it was easier to show differences between fibers and COC using natural specimens of the deep-sea coral *Lophelia pertusa,* (Rollion-Bard et al., 2003b; Blamart et al., 2005; Lutringer et al., 2005), or more recently of the zooxanthellate coral, *Colpophyllia* sp. (Meibom et al., 2006).

The first aim of this study was to characterize the isotopic signature of fibers and COC in the tropical coral *Acropora* sp., cultured under the controlled and constant conditions originally proposed by Marubini et al. (2003). As environmental conditions were kept constant, the observed variability may be due to biology. We examined the relationship between morphology and isotopic ratio. Our aim was to check if the "fusiform crystals" described by Gladfelter (1982) at the most distal parts of the growing tips of an *Acropora cervicornis* could be the same structures more recently described as COC. The isotope distribution noted was explained in light of the investigations dealing with kinetics and thermodynamics of bio-carbonate crystallization due to specific relationships between organic compounds and mineral. On the one hand, biologists have demonstrated that the formation of coral skeleton is influenced by symbiont metabolism and that the calicoblastic layer is involved in the secretion of an organic matrix (Gattuso et al., 1999; Allemand et al., 2004; Tambutté et al., 2007a,b for a review). On the other hand, atomic forcing microscopy (AFM) allowed the observation of surface processes during crystallization at the nanometer size scale (Reeder and Hochella, 1991; Paquette and Reeder, 1995; Teng et al., 1999). Previously it was shown that organic matter interacts with mineral and alters the equilibrium thermodynamics of the growth surface (Teng et al., 1998; De Yoreo and Velikov, 2003). Implications on interpretation of time series data devoted to climatic reconstruction is examined in the "conclusion".

2. MATERIAL AND METHODS

2.1. Material

Several small colonies of *Acropora verweyi* (Archaeocoeniina) were cultured following the procedure described by Reynaud-Vaganay et al. (1999), under constant and controlled conditions at different pH and then carbonate concentration according to Marubini et al. (2003). As such colonies grew glued onto glass slides. Aquaria were provided with light from overhead metal halide lamps (OSRAM H-QI 400 W) at an intensity of 300 ± 30 μmol m^{-2} s^{-1} for 12 h a day. Indeed, to ensure normal growth of symbiotic organism, irradiance followed a 12 h:12 h day:night cycle (Marubini et al., 2003). Seawater was heated to 26.5 °C (±0.2) using a 500 W heater (Rena) connected to an independent temperature controller (ElliWell PC 902/T). A small aquarium pump (Rena C20) ensured continuous water motion. Seawater renewal in the tanks was equal to 3 l per minute and was obtained from the flow-through system that pumps Mediterranean seawater from a depth of 50 m. Seawater $\delta^{18}O$ remained relatively constant both during a diurnal cycle (1.28‰ vs SMOW ± 0.01, $N = 3$) and during the course of the year (1.29 ± 0.01‰ vs SMOW, $N = 39$) (Reynaud-Vaganay et al., 1999). Corals experienced a constant pHSWS maintained at 8.061 ± 0.040, with constant alkalinity of 2635 ± 3 μeqkg^{-1} (Marubini et al., 2003).

2.2. Micro-structural characterization

Morphology of the microstructures was characterized by observations on a scanning electron microscope (SEM Philips 505) after gold/palladium coating of surfaces prepared by diamond polishing and ultra-light etching, according to the methods described by Cuif and Dauphin (1998).

2.3. Isotopic analysis

Ion probe oxygen isotope analyses were performed at CRPG-CNRS (Nancy, France) using the Caméca ims 1270 ion microprobe. The instrumental settings used are detailed in Rollion-Bard et al. (2007). The present experiment differs only in the size of the Cs^+ primary beam, which was 15 μm instead of 30 μm, without a decrease of analytical precision. A smaller beam size makes it easier to resolve the individual growth units earlier recognized in the skeleton. The size of the COC ranges between 5 and 10 μm, and as such is slightly smaller than the beam size. The fiber size is still smaller. Therefore, analysis of COC might include a few fibers and fiber samples are made of several fibers. Prior to analysis, the sample was polished using diamond paste down to 1-μm and coated with gold. The internal reproducibility was better than ±0.2‰ and the external reproducibility, based on repeated measurements

of standards, varied between 0.2‰ and 0.4‰ (1σ), depending on the session.

The $\delta^{18}O$ values were calibrated against the isotopic value given by conventional methods using an Optima-VG mass spectrometer. Results are given in the conventional (δ‰) notation expressed in per mil against the V-PDB standard (Vienna Pee Dee Belemnite), where:

$$\delta(\text{sample}) = (\text{Rsample} - \text{R Standard}) - 1) \times 10^3$$

Reproducibility for oxygen is ±0.05‰.

The data of the present experiment were compared with the equilibrium values of inorganic aragonite formed in the culture conditions. A temperature of 26.5 °C and water $\delta^{18}O$ equal to 1.28‰ vs V-SMOW (Reynaud-Vaganay et al., 1999). We calculated the equilibrium values for these conditions using O'Neil et al. (1969) and Kim and O'Neil (1997) who determined inorganic calcite temperature calibrations, taking into account the enrichment estimated for aragonite by Tarutani et al. (1969) and we obtained $\delta^{18}O_{V\text{-}PDB}$ values of −1.39‰ and −1.22‰, respectively. The same calculation has been made using Patterson et al. (1993) and Grossman and Ku (1986) equations determined for organic aragonite providing oxygen isotopic values of −1.12 and −0.37‰, respectively.

2.4. Statistical analysis

The data were analyzed using the program STATGRAF (StatPoint, Inc., USA). Non-parametric tests have been used in addition to the *t* test, because they have the advantage of avoiding assumption on the data distribution. Differences are significant at $p < 0.01$, and highly significant at $p < 0.001$.

3. RESULTS

3.1. Characterization of crystal units

Clearly, SEM observations showed two micro-structural components. Tiny crystals gathered into bundles and more massive COC. COC were rounded micro-crystals, 10–30 μm in diameter, randomly oriented. They were more or less accumulated or in continuous arrangement (Plate 1). Fibers were elongated mono-crystalline units, few microns in thickness or less. They seemed to be transversally cut by dark layers arranged like a growth layer, radiating from centers of calcification. The shape, size and orientation of COC and fibers clearly differed.

3.2. Sampling strategy

In the present study, the new skeleton, formed under controlled conditions, was grown on the glass slide, and sampled for the calibration of the growth units. COC-enriched zones were identified using SEM. To characterize the isotopic signature of fibers and COC, analyses were focused on the microstructures earlier characterized on the newly formed skeleton on two zones (Fig. 1a–c).

We then focused our measurements around the theca of the newly formed skeleton (Fig. 2) where Gladfelter (1982) recognized large amounts of "fusiform crystals", in order to highlight the nature of these mineral units. Indeed, coral skeleton is formed by a collection of tubes inhabited by individual organism called theca in which vertical sheets, called septae, radiated. The sampling of the septae aimed at confirming the presence of both COC and fibers as they have been identified from SEM observations (Cuif and Dauphin, 1998).

3.3. $\delta^{18}O$ measurement

In the newly formed skeleton (Fig. 1d and e), $\delta^{18}O$ values in the first zone analyzed ranged between −0.4‰ and −3.3‰ vs V-PDB for fibers and −4.3‰ and −5.4‰ for COC. In another zone (Fig. 1b and c), $\delta^{18}O$ values ranged between −2.1‰ and −3.9‰ for fibers and between −4.3‰ and −5.9‰ for COC. The isotopic ranges of each micro-structural unit measured in these two portions of *Acropora* were in good agreement, and $\delta^{18}O$ showed identical properties. Values were scattered in fiber-rich zones and they were almost constant in COC-rich zones, with values of -5.0 ± 0.3‰ (1σ) and -4.9 ± 0.4‰ (1σ), respectively (Fig. 1).

Samples collected around theca, ranged between -4.2 ± 0.3‰ and -6.3 ± 0.3‰ (1σ) and therefore showed the lowest isotopic values (Fig. 2). $\delta^{18}O$ of samples located along septae were more scattered, ranging from 0.0 ± 0.3‰ to -5.5 ± 0.3‰ (1σ) (Fig. 2).

After verifying data consistency (Table 1 and 2), all isotopic measurements were plotted on Fig. 3 according to their frequency of isotopic values. The total number of data was low for statistical analysis ($n = 64$) (Fig. 3a), never the less the distribution showed two distinct groups. The first one (39 colonies) was characterized by the lowest values (around −6‰ to −4‰) and the second one (25 colonies) had higher $\delta^{18}O$ values, ranging from −4‰ to 0.24‰. Taking into account measurement uncertainty, we noted that the highest measured $\delta^{18}O$ values differed by 1‰ from the isotopic equilibrium estimated at low SST by O'Neil et al. (1969) and Kim and O'Neil (1997) for inorganic aragonite (−1.39 and −1.22). These values were however, closer to those obtained by Patterson et al. (1993) and Grossman and Ku (1986) for organic aragonite (−1.12 and −0.37). Thus, Fig. 1 shows that COC isotopic signature was the lowest, and corresponded to the first group and the fiber values were scattered from quasi-equilibrium to COC values, and corresponded to the exponential-like decrease of the second group (Fig. 3a). Crystals measured around theca (Fig. 3b) were essentially composed of COC, while septa was constituted both of fibers and COC (Fig 3c). We noticed that the highest number of data corresponded to the boundary between values of COC and fibers.

Therefore, we conclude that even if some fiber contamination occurred in the COC due to spot size, the isotopic signature of COC was almost constant and equal to -5.0 ± 0.5‰. Fiber $\delta^{18}O$ values were highly variable but almost always lower than −0.37‰ (the maximal value of isotopic equilibrium, calculated for organic aragonite (Grossman and Ku, 1986)). Fiber $\delta^{18}O$ values were always

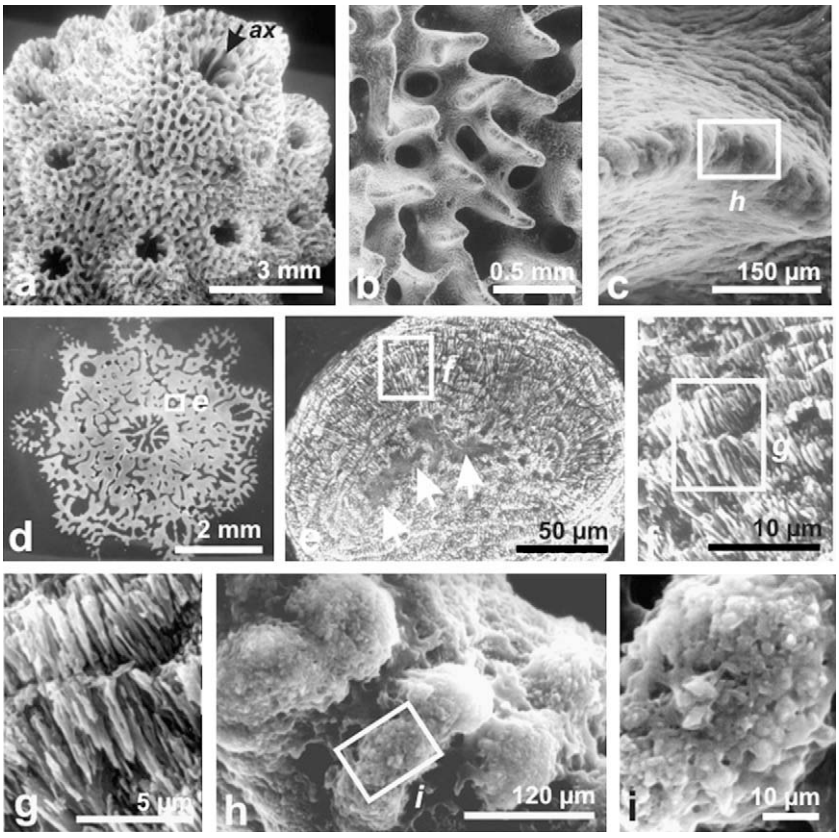

Plate 1. (a) Tip of an *Acropora* colony used for the growth experiments. Typical for the branching Acroporids colonies is the large sized axial corallite (*ax*), surrounded by smaller budding polyps. Compare to a transversal section in (d). (b and c) Between corallites, the skeletal tissue is made of anastomosed lamellae, each of them with typical corallian architecture. A median plan, the specific microstructure of which is well visible in (c) (cf. also (h–i)), is reinforced on both sides by superposed layers of fibrous tissue (cf. (f–g)). (d) Section perpendicular to the growth axis through a sample comparable to (a) Positions of the axial and secondary budding corallites are clearly exposed, as well as the importance of the inter-corallite skeleton. (e) Section of an inter-calicinal lamella perpendicular to the colony growth axis. The specific microstructure of the central part of the section is well exposed (arrows), surrounded by the concentric fibrous layers. (f–g) Fibrous tissues showing the layered mode of growth. (h–i) The specific microstructure of the early mineralization zones, at the growing distal areas of the septa and inter-calicinal lamellae. The crystallization process developed in these regions results in tiny crystals, randomly oriented, forming small densely packed nodules (the so-called centers of calcification = COC).

higher or equal to −5‰, compared to the COC isotopic signature.

4. DISCUSSION

The present study, confirms that there is a strong relationship between isotopic value, crystal shape and skeleton morphology. Crystals called "fusiform" by Gladfelter (1982), according to their shape, show the same isotopic values (19 data points on Fig. 3b) as COC. We distinguish in septa both COC (10 data) and fibers (12 data) (Fig. 3c). This confirms microscopic observations of septa (Cuif and Dauphin, 1998) showing discontinuous COC surrounded by fibers.

Low isotopic values, as those observed in Figs. 1 and 2, could have been due to contamination by some organic matter. Indeed, organic matter is intimately associated with the mineral (Gaffey, 1988; Cuif et al., 1999; Tambutté et al., 2007a,b, for a review). Coral organic matter isotopic composition usually ranges from −13‰ to −20‰ (Grottoli et al., 2005) and can affect aragonite $\delta^{18}O$ by depleting it. However, no organic matter has been observed by SEM because its amount is low compared to the mineral fraction, estimated to vary from 0.01% (Constanz and Weiner, 1988) of the total dry skeleton weight (Wainwright, 1963), to 0.6% (Boiseau and Juillet-Leclerc, 1997) and 2.5% when internal water is included (Cuif et al., 2004). Moreover, when there is a contamination by organic matter in oxygen isotopic measurements by ion microprobe (Rollion-Bard et al., 2003b), there is a relation between oxygen intensity and $\delta^{18}O$ values, which is not observed here. Therefore, we conclude that organic matter was not an important contaminant in our measurements. The absence of organic matter observed by SEM also eliminated contamination by fungi or micro-boring organisms (McIntyre and Towe, 1976; Le Campion-Alsumard et al., 1995; Nothdurft et al., 2007a).

This study differs from earlier published papers dealing with isotope micro-measurements (Rollion-Bard et al., 2003a,b; Meibom et al., 2006) in that the analyses were

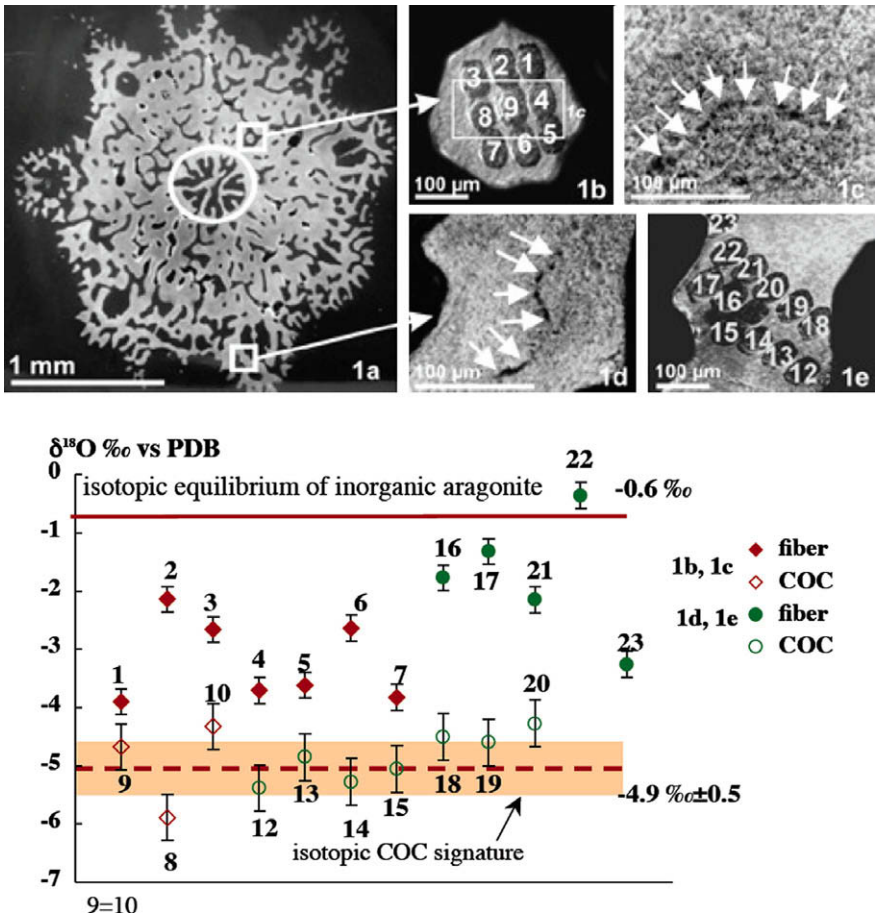

Fig. 1. SEM observations of the cultured *Acropora* skeleton. (a) View of the newly formed skeleton. The white circle highlights the initial nubbin location. Two closely imaged regions are focused (c and d) and show COC underlined by white arrows localized by a slight etching. The remaining skeleton is formed by fibers. The numbers on (b and d) corresponds to ion probe spots plotted on (f) (#10 is a duplicate of #9). On (f), $\delta^{18}O$ are plotted versus the sample number. $\delta^{18}O$ measured from COC are the lowest and almost constant, while the $\delta^{18}O$ values of the fibers are scattered between the isotopic equilibrium value and the COC isotopic signature.

performed on aragonite deposited in controlled and quasi-constant conditions. The difference between the consistency in the isotopic signal of rounded crystal and the scattering of the fiber signal lead us to conclude that each crystalline microstructure shows a specific isotopic signature. In addition, constant COC $\delta^{18}O$ suggest that, it could only vary with environmental factors even though its absolute value is in isotopic disequilibrium and affected by biomediation of aragonite. In opposite, inherent fiber $\delta^{18}O$ variability can be regarded as biological influence.

4.1. COC and fibers identification

In another coral species, *Colpophyllia* sp., (Meibom et al., 2006) have also measured a lower $\delta^{18}O$ signal in COC than in fibers. We agree with these authors who concluded that COC were deposited out of equilibrium. As in our experiment, *Acropora* colonies were cultured under a constant environment, as such we can compare the $\delta^{18}O$ distribution in *Acropora* with the distribution observed in deep-sea corals, which also grow under constant conditions, such as *Lophelia pertusa* (Rollion-Bard et al., 2003b; Lutringer et al., 2005), or other deep-sea coral skeleton, *Despophyllum cristagalli* (Adkins et al., 2003). COC constitute trabecula both in deep-sea and tropical corals (Nothdurft and Webb, 2007b) and $\delta^{18}O$ distribution (ranging between COC and fibers values) is identical for both coral genera. Thus, high scattering of fiber $\delta^{18}O$ is not only inherent to tropical corals but also to those found in the deep sea. The existence of two types of crystals deposited following distinct processes would be a property common to all coral genera.

In the study by Adkins et al. (2003), COC and fiber crystals were not distinguished, thus, in order to combine high $\delta^{18}O$ variability (strongly correlated with $\delta^{13}C$) and low $\delta^{18}O$ off the linear $\delta^{18}O$ and $\delta^{13}C$ trend, appearing like the lowest limit, they were obliged to assume that all crystals were formed following a single mechanism. This led them to assume that kinetics could not control isotopic fractionation, as Smith et al. (1997, 2000) claimed it. They rather suggested that $\delta^{18}O$ was biologically induced through a pH gradient associated with the presence of respired CO2 (Adkins et al., 2003). If we assume that the mechanisms of COC and fiber deposition and the

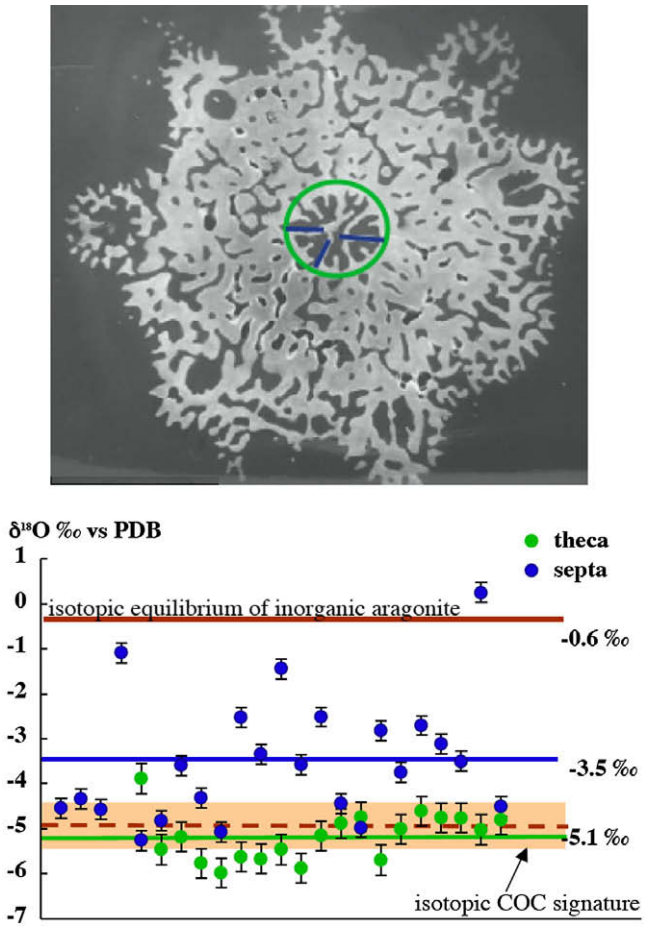

Fig. 2. The oxygen isotopic values measured around the growing tips (underlined by green circle) of *Acropora,* where Gladfelter (1982) recognized fusiform crystals, indicate that they have a close isotopic signature (-5 ± 0.3‰) to that of COC (-4.9 ± 0.4‰) identified on the newly formed crystal. Samples from septae (in blue) reveal both scattered low values specific to COC and isotopic values measured on fibers, which ranged from the equilibrium value to the limit defined by COC, as was expected (Cuif and Dauphin, 1998). (For interpretation of the references to color in this figure legend, the reader is referred to the web version of this paper.)

Table 1
Range of oxygen isotopic composition of the skeleton microstructures on cultured Acropora. *N* is the number of analyzes, *m* the mean values, σ the standard deviation.

	All	*Acropora*				*Lophelia*	
		FIBERS	COC	SEPTA	THECA	FIBERS	COC
N	65	12	10	23	20	17	16
m	−4.0	−2.6	−4.9	−3.5	−5.0	0.7	−2.6
σ	1.4	1.1	0.5	1.3	0.6	2.2	1.2
Max	0.2	−0.4	−4.3	−0.2	−3.9	4.4	1.1
Min	−6.0	−4.0	−6.0	−5.3	−6.0	−3.0	−4.5
Mode	−5.5	−3.3	−5.1	−3.7	−5.5	−0.5	−2.8

associated isotopic fractionations differs, it is possible to separate crystals showing high $\delta^{18}O$ and $\delta^{13}C$ values from those characterized by variable low $\delta^{13}C$ and $\delta^{18}O$ values, as they have been described by Adkins et al. (2003). By assuming that $\delta^{11}B$ is a pH proxy, $\delta^{11}B$ measurements in *Lophelia pertusa* (deep-sea coral) microstructures (Blamart et al., 2007) demonstrated that internal pH calculated for COC was not that expected by Adkins et al. (2003). Indeed, the model developed by Adkins et al. (2003) supposed that COC were deposited under high pH conditions, whereas measurements indicated low ones (Blamart et al., 2007). Therefore, $\delta^{18}O$ and $\delta^{13}C$ correlation observed in the less dense skeleton portion of deep-sea coral skeleton corresponds to the portion of the skeleton rich in fibers (Adkins et al., 2003; Rollion-Bard et al., 2003b; Lutringer et al., 2005). While our data derived from tropical coral fiber do

Table 2
Results of the *t*-test (Student's test) and two non-parametric tests: KS (Kolmogorov–Smirnov) and Mann–Whitney test. All the tests are highly significant.

	Acropora		*Lophelia*
	FIBERS/COC	THE/SEPT	FIBERS/COC
t	HS	HS	HS
KS	HS	HS	HS
Mann–Whitney	HS	HS	HS

not include $\delta^{13}C$ measurements, nothing prevents us from agreeing with the kinetic precipitation for deep-sea corals. This similarity between symbiotic and non-symbiotic corals could compromise the assumption of an active role of photosynthesis in determining isotopic fractionation (Rollion-Bard et al., 2003a).

4.2. The kinetic assumption

High scattering of isotopic and trace element data in fibers has previously been described (Rollion-Bard et al., 2003a,b; Meibom et al., 2004, 2006, 2007; Cohen and McConnaughey, 2003). Rollion-Bard et al. (2003a) gave a first explanation of the high $\delta^{18}O$ scattering using a symbiotic coral (*Porites lutea*) and $\delta^{11}B$ measurements by ion microprobe. $\delta^{11}B$ values indicated that internal pH, between calicoblastic cells and skeleton could vary between 7.1 and 9, which are in good agreement with local measurements performed under light and dark conditions (Al-Horani et al., 2003). To calculate deposit duration, which would agree with the measured $\delta^{11}B$–$\delta^{18}O$ values, the oxygen ratio ranging from "initial disequilibrium with H2O" to isotopic equilibrium, Rollion-Bard et al. (2003a) supposed that aragonite was deposited in thermodynamic equilibrium and thus, used equilibrium constants.

Precipitation duration was thus estimated to be at least 1 h. This disagrees with the radioactive labeling measurements performed by biologists. Skeleton precipitation in a solution containing ^{45}Ca demonstrated that radioactive atoms were incorporated after only a few minutes (Tambutté et al., 1995, 1996; Furla et al., 2000). This confirms that, in opposite with what is suggested by Rollion-Bard et al. (2003a), $\delta^{18}O$ fiber scattering does not need pH change related to photosynthesis activity and that $\delta^{18}O$ fiber distribution in symbiotic and asymbiotic corals may be similar.

However, some portions of the skeleton may be slowly deposited (Raz-Bahat et al., 2006), and internal pH may play a prominent role in isotopic fractionation. We therefore agree with McConnaughey (1989b, 2003), Cohen and McConnaughey (2003), Sinclair (2005), Allison et al. (2005), Gaetani and Cohen (2006), and Rollion-Bard et al. (2003a) who favored a kinetic process for coral skeletogenesis. The isotopic oxygen disequilibrium of COC derived from the present study and the one performed by Meibom et al. (2006) seems to disagree with experiments showing that COC Sr/Ca corresponds to the equilibrium value (Cohen et al., 2001; Cohen and McConnaughey,

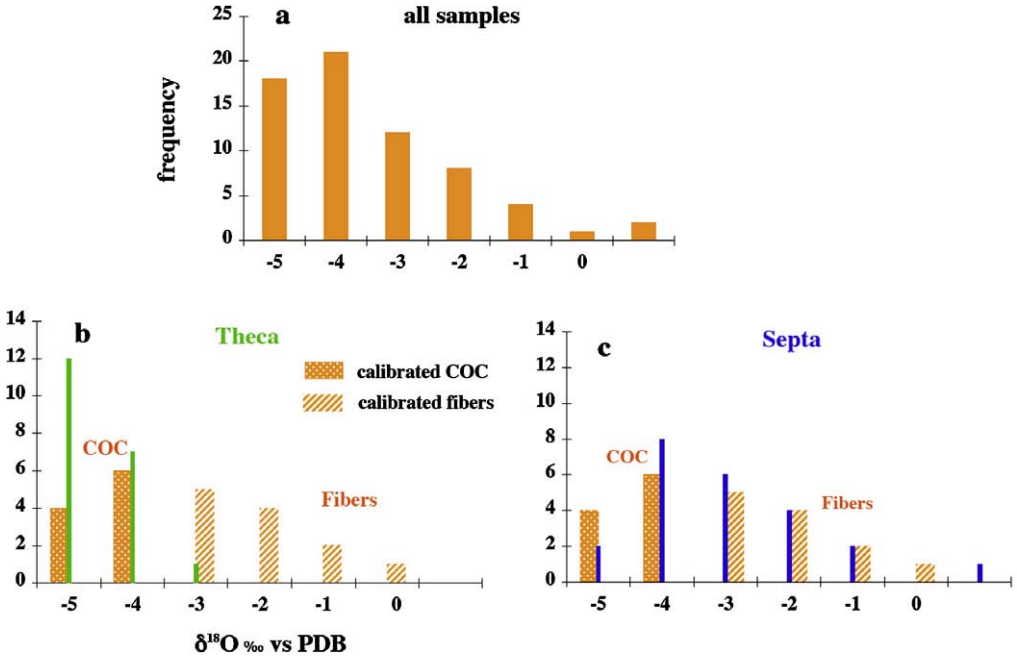

Fig. 3. Histogram of $\delta^{18}O$ values: the number of measurements is plotted versus their isotopic ranges, from −6‰ to −5‰ and from 0‰ to 1‰. On a) all the data are plotted, showing high number of low values (between −6‰ and −4‰). From this value, the number of higher values is decreasing until a value close to isotopic equilibrium. The higher number of low $\delta^{18}O$ compared to the others is an artefact due to sampling. On (b) and (c) the values measured around the theca (green) and septa (blue) are compared with the calibrated data. We infer that the theca is essentially formed by COC, while the septae consists of the mixture of both COC and fibers. (For interpretation of the references to color in this figure legend, the reader is referred to the web version of this paper.)

2003). However, biological investigations using ^{85}Sr on *Stylophora pistillata* have demonstrated that incorporation of Sr^{2+} is inversely correlated with the rate of calcification (Ferrier-Pagès et al., 2002). Thus, the maximal disequilibrium degree for aragonite could correspond with Sr/Ca equilibrium, which is consistent with kinetic assumption. This indicates that in order to interpret the chemical signature of coral skeleton the incorporation mode of each element needs to be taken into account, which is strongly controlled by biology. As such the present discussion will be only focused on the oxygen isotopic ratio. Other experiments including trace elements and stable isotopes would be necessary to make further conclusions (Shirai et al., 2008).

COC of cultured *Acropora* are deposited in the highest degree of isotopic and thermodynamic disequilibrium (Zeebe and Wolf-Gladrow, 2001) and their $\delta^{18}O$ variability depends only upon external factors while fibers experience all kinetic conditions (from the highest degree of disequilibrium to the equilibrium), without any relationship with external forcing. We must explain how two close crystals may be precipitated following distinct patterns.

4.3. Biomineralization

We cannot explain the existence of two mineral deposition processes and intrinsic high variability of chemical data observed in coral skeleton without taking into account new biological advances. Conversely to the common geochemist concept for which coral skeleton formation is a chemically dominated process, biologists argue in favor of a biologically controlled biomineralization (Goreau, 1959; Johnston, 1980; Lowenstam and Weiner, 1989; Allemand et al., 2004). Newly formed coral aragonite is deposited at the interface between the calicoblastic layer and the skeleton (Allemand et al., 2004). Biologists using ^{14}C labeled molecules and a pharmacological approach suggested that a prerequisite step of calcification could be the organic matrix biosynthesis (Wainwright, 1963; Young et al., 1971; Allemand et al., 1998). Though modalities of formation and transport of organic matrix compounds are not totally understood, calicoblastic cells should play a determinant role in this phase of calcification (Goreau, 1959; Johnston, 1980; Puverel et al., 2005). The intimate relationship between coral tissue anchored to skeleton by specialized cells called desmocytes and organic matrix, is well highlighted by immunolabeling with antibodies (Tambutté et al., 2007a,b). Unfortunately, among molecules constituting the organic matrix, only galaxin has been identified (Fukuda et al., 2003).

By observing fiber arrangement on Plate 1 we notice that the needle-like crystals oriented in the same direction and arranged in successive layers around COC, strongly differ from crystalline organization shown by an inorganic mineral (Goreau, 1959; Johnston, 1980). These features are recognized characteristics of mineralization performed under organic control (Mann et al., 1993). Investigations conducted in mineralogy, at crystal scale, using AFM (Reeder and Hochella, 1991; Paquette and Reeder, 1995; Teng et al., 1999) demonstrated that calcite precipitated in the presence of aspartic acid, abundantly present in coral organic matrix (Allemand et al., 1998; Cuif et al., 1999; Grassmann et al., 2003), lead to crystallization governed by thermodynamic disequilibrium. Indeed, Teng et al. (1998) demonstrated that: "the primary effect of aspartic acid on crystallization is to alter the equilibrium thermodynamics of the growth surface". Therefore, the presence of organic molecules in proximity to the coral skeleton could explain why the mineral formation is in chemical disequilibrium and thus, in isotopic disequilibrium.

4.4. Possible origin of the dual isotopic fractionation

The organic matrix strongly linked to the skeleton is well preserved through time. For example, $\delta^{15}N$ isotopic signature of organic matrix allowed Muscatine et al. (2005) to demonstrate that a Triassic coral was symbiotic. Skeleton AFM observations revealed that the organic matrix coated the 50–100 nanometer grains that built crystals in COC and fiber bundle (Dauphin, 2001; Cuif and Dauphin, 2005). Moreover, investigations using XANES (X-ray Absorption Near Edge Spectrum) at high resolution (sub-micron) make it possible to separate two states of organic sulfate, one in the organic matrix coating COC and another one in matrix surrounding fiber bundles (Cuif et al., 2003). This indicates that compounds of organic matrix differ following the type of crystal coated. Recent nano-SIMS measurements of carbon and sulfur supported this observation (Meibom et al., 2007). The discrepancy of a chemical environment surrounding each crystal type might induce different deposition processes. Therefore, the organic matrix might be responsible for the precipitation of COC versus fibers and their different isotopic fractionation. Such hypothesis needed to suppose that COC are totally isolated from fibers (Meibom et al., 2006) as shown between each fiber bundle (Tambutté et al., 2007a,b).

The hypothetical concepts of a "common carbon pool" (Goreau, 1977) or later of "a calcifying fluid" (McConnaughey, 1989a,b; Swart et al., 1996; Adkins et al., 2003; Cohen and McConnaughey, 2003), created for justifying metabolic impact on skeleton, are not consistent with such an assumption.

Due to a lack of evidence, we cannot infer a more precise deposition mechanism of COC than an extreme isotopic disequilibrium. Although COC isotopic signature is similar to the lowest isotopic values shown by fibers, we cannot assimilate their respective deposition mechanism. Indeed, the great discrepancy of their shape indicates that they have strongly different formation processes.

4.5. Fiber deposition

Although the studied coral species and the derived calcification models differ following the authors, Gladfelter (1982), Barnes and Lough (1993), Cuif and Dauphin (1998), Raz-Bahat et al. (2006) suggested that aragonite deposition is operated at least into two stages. First COC, (or fusiform crystals) are deposited and form a framework, which is reinforced in a second stage by needle-like crystals. The model proposed by Raz-Bahat et al. (2006) is more

complex but there are still two growth steps: One associated with coral tissue expansion and the other one associated with skeleton accretion. We notice that these latter authors suggested an intrinsic process controlling skeletogenesis even in the absence of photosynthesis. This is in agreement with our earlier remark stressing that the high $\delta^{18}O$ scattering of fibers was both observed on symbiotic (Rollion-Bard et al., 2003a; Meibom et al., 2006) and non-symbiotic corals (Rollion-Bard et al., 2003b; Adkins et al., 2003; Lutringer et al., 2005).

Observation and comparison of coral tissue (after decalcification) and skeleton microstructures of *Stylophora pistillata,* using Field Emission Scanning Electron Microscopy (FESEM), underlined a strong morphological correspondence between soft tissue and skeleton (Tambutté et al., 2007a,b). Even at the microscopic level, calicoblastic cells (shown to secrete organic matrix) correspond exactly to the shape of fiber bundles, horizontally or vertically distributed (Tambutté et al., 2007a,b). Such a compartment-like structure had been yet observed on other coral species (Johnston, 1980; Brown et al., 1983; Gladfelter, 1983; Golberg, 2001). Each fiber bundle would be individualized by organic matrix network-like.

This could suggest that fibers contained in a single bundle are formed in a volume more or less isolated by organic molecules. Under these conditions the main external control of fiber formation of a single bundle could result in the supersaturation of calcium carbonate in such an individualized volume (De Yoreo and Velikov, 2003). By supposing that fibers are deposited according to this model, the high $\delta^{18}O$ variability would be due to fluctuation of mineral growth rate induced by the organic environment (De Yoreo and Velikov, 2003) and controlled by physical and chemical conditions, created by metabolic activity inside the organism. Photosynthetic activity may also contribute to isotopic variation by creating specific chemical conditions such as pH. The aragonitic nature of the coral skeleton does not change our assumptions.

The low $\delta^{18}O$ data of COC and the lowest values shown by fibers could correspond to the "initial disequilibrium with H2O" implied by an "instantaneous" deposit (Rollion-Bard et al., 2003a; McConnaughey, 2003). Fig. 3 shows that the isotopic range between the two limits mentioned earlier is covered by our data and could indicate that calcification rate varies from instantaneous formation to rate necessary to reach equilibrium. Deposition rate variations could drive to isotopic scattering, which covers all degrees of disequilibrium.

Raz-Bahat et al. (2006) observed on growing *Stylophora* this high variability of deposition rate. However, it is important to underline that the kinetics of crystal growth is not directly related to calcification rates characterized at higher size scales, such as calcification or the amount of aragonite deposited and linear extension of the corallites per time unit, combined to determine skeleton density (Lough and Barnes, 2000). Allison and Finch (2004), by measuring and comparing Sr/Ca microstructure distribution in layers grown at different extension rates demonstrated that there were no noticeable differences in COC and fibers chemical signatures. Naturally, the time units of skeleton thickening by fibers or elongation ensured by COC (Plate 1) (Nothdurft and Webb, 2007b) and density bands formation are not of the same order.

$\delta^{18}O$ values correspond to deposition rates from instantaneous to equilibrium precipitation. This suggests that there is a limiting factor implying a progressive depletion of supersaturation conditions and thus of deposition rate. We have to suppose that there is a finite concentration of Ca^{2+} or CO_3^{2-} the "individual fiber bundle" volume.

4.6. The sub-calicoblastic space: a still obscure concept

Although numerous observations have been carried out on several coral species, using different techniques, the calcifying fluid concept still remains poorly understood: Nothing is known about its composition and the interface between the calicoblastic layer and the skeleton appears too small to contain any fluid (Allemand et al., 2004; Tambutté et al., 2007a,b; Meibom et al., 2008).

The mechanism of calcium transport from seawater to the calicoblastic ectoderm is still a matter of debate. It is generally suggested that the transepithelial calcium transport involves at least one transcellular pathway across the calicoblastic epithelium as the site of active transport (Tambutté et al., 1996; Marshall, 1996; Allemand et al., 2004). In addition, Ca^{2+} ATPase is assumed to play an active role in calicoblastic cells (McConnaughey and Whelan, 1997; Zoccola et al., 2004). Clode and Marshall (2003) using FESEM and X-ray microanalysis, observed nodules possibly corresponding with Ca-rich region in close proximity to the calicoblastic cells and thus to the organic matrix. It is indeed well known that proteins isolated from sites with biomineralization notably negatively charged aspartic acid-rich molecules, are preferentially bound to cations such as Ca^{2+} by electrostatic interactions (Weirzbicki et al., 1994; Shin et al., 2000). Thus, amino-acid side chains are known to mediate specific interactions with calcite steps and surfaces (Addadi and Weiner, 1985; Orme et al., 2001; Elhadj et al., 2006).

In order to ensure the supersaturation of the calcification site, and to allow for rapid deposition of the framework deposited for newly formed skeleton (Gladfelter, 1982; Barnes et al., 1993; Raz-Bahat et al., 2006), $HCO_3^-$and CO_3^{2-}need to be transported to the skeleton-calicoblastic interface. Specific carriers would allow a faster and regulated transport of HCO_3^- and CO_3^{2-} towards the extracellular calcifying medium, the relative ionic distribution being regulated by H^+ transport (for example the Ca^{2+}-ATPase which is a Ca^{2+}/H^+ exchanger, Cohen and McConnaughey, 2003). In addition, the majority of the carbon (70%) used for CaCO3 formation may originate from respired CO2 (Erez, 1978; Furla et al., 2000). Futhermore, carbonic anhydrase is thought to facilitate calcification by removing CO2 after CaCO3 deposition (Goreau (1959) or by speeding up CO2 conversion into CO_3^{2-}close to calicoblastic layer (Tambutté et al., 1986; Furla et al., 2000; Al-Horani et al., 2003) or by regulating internal pH (Al-Horani et al., 2003; Moya et al., 2006). However, since DIC is used both for photosynthesis and calcification, the inter-relation is complex (Allemand et al., 2004). We maintain that an active mechanism of trans-

port should be involved to supply carbon to the site of calcification as the supersaturation condition is necessary.

Bone or dentin phosphate is a biomineral that is much more documented than coral skeleton. This material has showed that mineral precipitation might occur in a small area as pores existing between molecules of organic network (Veis, 2003). In these conditions there is a strong similarity between shapes of organic framework and the skeleton, similar with what has been observed by FESEM on the *Stylophora pistillata* skeleton (Tambutté et al., 2007a,b).

In asserting that Ca^{2+} and/or carbon species would be confined by organic matrix macromolecules in small quantities, there may be sufficient amounts to initiate "instantaneous" crystallization. If Ca^{2+} and/or carbon species are not renewed, the supersaturation conditions deplete, which lead to the decrease of deposition rate and thus, an isotopic fractionation of fibers kinetically controlled. Many conditions remain to be checked to confirm such a scenario, but this is consistent with our present understanding of coral biology, the process of the mineralization of its skeleton and our isotopic data.

To summarize coral biomineralization: Oxygen isotope analyses of skeleton microstructures shed in light how chemical and/or physical processes might be adapted by biology to form crystals characterized by specific shapes and distributed following a hierarchical arrangement. In the case of coral skeleton, aragonite crystal deposition is controlled by surface reactions created by organic matrix. Mineral precipitation adheres to supersaturation law and isotopic fractionation is controlled by the rate of the deposition depending upon local chemical environment related both to metabolic activity and environmental parameters.

The present study, stresses that vital effect is not restricted to a bias added to inorganic aragonite isotopic ratio by coral metabolic activity but we demonstrated that the presence of organic molecules has the capability to control the mineral deposition mechanism. Moreover, the nature and the relative amounts of these organic molecules are able to modulate geochemical response. Probably, the influence of external factors is superimposed on the chemical signature of coral biomineral genetically determined.

5. CONCLUSIONS: CONSEQUENCES ON CLIMATIC STUDIES

The main vital effect highlighted by this study corresponds to the offset in the isotopic composition of coral skeleton relative to the equilibrium with seawater. Indeed, these samples are made of heterogeneous mineral microstructures. The measured macro-sample $\delta^{18}O$ results from the integration of highly scattered isotopic values influenced by both biological and external factors. As it has been demonstrated by Rollion-Bard et al. (2003a), the macro-measurement is the average of values almost only including $\delta^{18}O$ lower than the isotopic equilibrium, which explains the systematic negative offset presented by isotopic macro-sample values. The potential heterogeneity of subsamples also justifies the low reproducibility of coral samples compared with standards.

The measured macro-sample $\delta^{18}O$ also depends upon the relative proportion of COC and fibers. This could justify that $\delta^{18}O$ versus SST calibrations calculated from annual measurements performed on several specimen differ according to taxonomy (Weber and Woodhead, 1972). This also offers an explanation regarding the isotopic variability shown by different morphologic parts of the skeleton (Land et al., 1975).

We noticed that micro-measurement significance could not be compared with that of a sample collected at millimeter scale. The isotopic value derived from thin growth layers similar with the microstructure shown on Plate 1, likely does not indicate conditions prevailing in seawater but rather provide information about the internal conditions created at this specific location of skeleton and by biological activity at the time of precipitation. Chemical data becomes relevant in terms of external variability when measurements integrate a long enough time sequence as well as fragments large enough to partially remove variability due to biology and morphology. Monthly periodicity exhibited by micro-samples collected following a linear profile of a "wild" coral by $\delta^{18}O$ measurements (Rollion-Bard et al., 2003a) as well as by Sr/Ca analysis (Meibom et al., 2003) could indicate that sample data representing one month is the limit to get relevant information in term of environmental indicator. In the present study, we demonstrated that the chemical value used as climate proxy at macro-size scale might provide at the micro-size scale, vital information about the deposition process of the crystals. We highlighted that the chemical process prevailing during fiber coral skeleton deposition is a kinetic one. In the *Porites* skeleton this crystal type prevails, however this is not consistent with the commonly accepted assumptions made by geochemists. We have now to explain how macro-samples collected along the main growth axis of a massive coral head seem to adhere to SST following a quasi-isotopic equilibrium with seawater.

We demonstrated that several factors of biological and environmental origins are potentially capable to affect chemical measurements conducted on coral skeleton, and as such, climatic reconstructions should be derived from multi-proxy data using more complex relationships than linear empirical equations. According to this rationale, we applied neural networks to multi-proxy time series and reconstructed accurate sea surface temperature and salinity variability, back in time (Juillet-Leclerc et al., 2006). This method has the capability to decipher from several proxy data series measured on a single aragonite sample, for each environmental factor, the portion of the signal due to environment and the portion caused by biological activity. As sampling is performed continuously along similar corallites, the biological filter remains the same during the time. This reconstruction proves that by taking into account biologic specificities of coral skeleton we keep considering coral as the best tropical climate recorder.

ACKNOWLEDGMENTS

The national program ECLIPSE (Environnement et CLImat du Passé: hiStoire et Evolution) supported this study. The authors

thank T. McConnaughey, A. Meibom, N. Frank and anonymous reviewers for fruitful contributions, which significantly improved the quality of the paper. This work benefited greatly from the encouraging and constructive Dr Lyon (associate Editor) comments. Additional thanks to Cecilia Garrec for English-language editing.

REFERENCES

Addadi L. and Weiner S. (1985) Interactions between acidic proteins and crystals: stereochemical requirements in biomineralization. *Proc. Natl. Acad. Sci. USA* **82**, 4110–4114.

Adkins J. F., Boyle E. A., Curry W. B. and Lutringer A. (2003) Stable isotopes in deep-sea corals and a new mechanism for "vital effects". *Geochim. Cosmochim. Acta* **67**, 1129–1143.

Al-Horani F., Al-Moghrabi S. A. and de Beer D. (2003) Microsensor study of photosynthesis and calcification in the scleractinian coral, *Galaxea fascicularis*: active internal carbon cycle. *J. Exp. Mar. Biol. Ecol.* **288**, 1–15.

Allemand D., Tambutté É., Girard J.-P. and Jaubert J. (1998) Organic matrix synthesis in the scleractinian coral *Stylophora pistillata*: role in biomineralization and potential target of the organotin tributyltin. *J. Exp. Biol.* **201**, 2001–2009.

Allemand D., Ferrier-Pagès C., Furla P. F., Houlbrèque F., Puverel S., Reynaud S., Tambutté E., Tambutté S. and Zoccola D. (2004) Biomineralisation in reef-building corals: from molecular mechanisms to environmental control. *C.R. Palevol* **3**, 453–467.

Allison N. and Finch A. A. (2004) High-resolution Sr/Ca records in modern *Porites lobata* corals: effects of skeletal extension rate and architecture. *Geochem. Geophys. Geosyst.* **Q05001**. doi:10.1029/2004GC000696.

Allison N., Finch A. A., Newville M. and Sutton S. R. (2005) Strontium in coral aragonite: 3. Sr coordination and geochemistry in relation to skeletal architecture. *Geochim Cosmochim. Acta* **69**, 3801–3811. doi:10.1016/j.gca.2005.01.026.

Barnes D. J. and Lough J. M. (1993) On the nature and causes of density banding in massive coral skeletons. *J. Exp. Mar. Biol. Ecol.* **167**, 91–108.

Blamart D., Rollion-Bard C., Cuif J.-P., Juillet-Leclerc A., Lutringer A., van Weering T. and Henriet J.-P. (2005) C and O isotopes in a deep-sea coral (*Lophelia pertusa*) related to skeletal microstructure. In *Cold-water Corals and Ecosystems* (eds. A. Freiwald and J. M. Roberts). Springer-Verlag, Berlin Heidelberg, pp. 1005–1020.

Blamart D., Rollion-Bard C., Meibom A., Cuif J.-P., Juillet-Leclerc A. and Dauphin Y. (2007) Correlation of boron isotopic composition with ultrastructure in the deep-sea coral *Lophelia pertusa*: Implications for biomineralization and paleo-pH. *Geochem. Geophys. Geosyst.* **8**, Q05001. doi:10.1029/2007GC001686.

Boiseau M. and Juillet-Leclerc A. (1997) H_2O_2 treatment of recent coral aragonite: oxygen and carbon isotopic implications. *Chem. Geol.* **143**, 171–180.

Brown B. E., Hewit R. and Le Tissier M. A. A. (1983) The nature and construction of skeletal spines in *Pocillopora damicornis*. *Coral Reefs* **2**, 81–89.

Clode P. L. and Marshall A. T. (2003) Skeletal microstructure of *Galaxea fascicularis* exsert septa: a high resolution SEM study. *Biol. Bull.* **204**, 146–154.

Cohen A., Layne G. D., Hart S. R. and Lobel P. S. (2001) Kinetic control of skeletal Sr/Ca in a symbiotic coral: implications for the paleotemperature proxy. *Paleoceanography* **16**, 20–26.

Cohen A. and McConnaughey T. (2003) Geochemical perspectives on coral mineralization. In *Reviews in Mineralogy and Geochemistry Volume 54 "Biomineralization"* (eds. P. M. Dove, J. J. deYoreo and S. Weiner). Mineralogical Society of America, pp. 151–187.

Cole J. E., Fairbanks R. G. and Shen G. T. (1993) Recent variability in the Southern Oscillation: isotopic results from a Tarawa Atoll coral. *Science* **260**, 1790–1793.

Constanz B. and Weiner S. (1988) Acidic macromolecules associated with the mineral phase of scleractinian coral skeleton. *J. Exp. Zool.* **248**, 253–258.

Cuif J.-P. and Dauphin Y. (1998) Microstructural and physico-chemical characterisation of centres of calcification in septa of some Scleractinian corals. *Pal Zeit* **72**, 257–270.

Cuif J.-P., Dauphin Y., Freiwald A., Gautret P. and Zybrowius H. (1999) Biochemical marker of zooxanthellae symbiosis in soluble matrices of skeleton of 24 *Scleractinia* species. *Comp. Biochem. Physiol.* **123A**, 269–278.

Cuif J.-P., Dauphin Y., Doucet J., Salome M. and Susini J. (2003) XANES mapping of organic sulphate in three Scleractinian coral skeletons. *Geochim. Cosmochim. Acta* **67**, 75–83.

Cuif J.-P., Dauphin Y., Berthet P. and Jegoudez J. (2004) Associated water and organic compounds in coral skeletons: quantitative thermogravimetry coupled to infrared absorption spectrometry. *Geochem., Geophys, Geosyst.* **5**, Q11011. doi:10.1029/2004GC000783.

Cuif J.-P. and Dauphin Y. (2005) The Environment recording unit in coral skeletons, a synthesis of structural and chemical evidences for a biochemically driven, stepping-growth process in fibres. *Biogeosciences* **2**, 61–73.

Dauphin Y. (2001) Comparative studies of skeletal soluble matrices from some scleractininan corals and Molluscs. *Biol. Macromol.* **28**, 293–304.

De Yoreo J. J. and Velikov P. G. (2003) Principles of crystal nucleation and growth. In *Reviews in Mineralogy and Geochemistry Volume 54 "Biomineralization"* (eds. P. M. Dove, J. J. DeYoreo and S. Weiner). Mineralogical Society of America, pp. 57–93.

Dunbar R. B., Wellington G. M., Colgan M. W. and Glynn P. W. (1994) Eastern Pacific sea surface temperature since 1600 A.D.: the $\delta^{18}O$ record of climate variability in Galapagos corals. *Paleoceanography* **9**, 291–315.

Elhadj S., De Yoreo J. J., Hoyer J. R. and Dove P. M. (2006) Role of molecular charge and hydrophilicity in regulating the kinetics of crystal growth. *Proc. Natl. Acad. Sci. USA* **103**, 19237–19242.

Erez J. (1978) Vital effect on stable-isotope composition seen in foraminifera and coral skeletons. *Nature* **273**, 199–202.

Ferrier-Pagès C., Boisson F., Allemand D. and Tambutté É. (2002) Kinetics of strontium uptake in the scleractinian coral *Stylophora pistillata*. *Mar. Ecol. Prog. Ser.* **245**, 93–100.

Fukuda I., Ooki S., Fujita T., Murayama E., Nagasawa H., Isa Y. and Watanabe T. (2003) Molecular cloning of a cDNA encoding a soluble protein in the coral exoskeleton. *Biochem. Biophys. Res. Commun.* **304**, 11–17.

Furla P., Galgani I., Durand I. and Allemand D. (2000) Sources and mechanisms of inorganic carbon transport for coral calcification and photosynthesis. *J. Exp. Biol.* **203**, 3445–3457.

Gaetani G. A. and Cohen A. L. (2006) Element partitioning during precipitation of aragonite from seawater. A framework for understanding paleoproxies. *Geochim. Cosmochim. Acta* **70**, 4617–4634.

Gaffey S. (1988) Water in skeletal carbonates. *J. Sedim. Petrol.* **58**, 397–414.

Gattuso J.-P., Allemand D. and Frankignoulle M. (1999) Photosynthesis and calcification at cellular, organismal and community levels in coral reefs: a review on interactions and control by carbonate chemistry. *Amer. Zool.* **39**, 160–183.

Gladfelter E. H. (1982) Skeletal development in *Acropora cervicornis*: I. Patterns of calcium carbonate accretion in the axial corallite. *Coral Reefs* **1**, 45–51.

Gladfelter E. H. (1983) Skeletal development in *Acropora cervicornis*: II. Diel patterns of calcium carbonate accretio. *Coral Reefs* **2**, 91–100.

Golberg W. M. (2001) Acid polysaccharids in the skeletal matrix and calicoblastic epithelium of the stony coral. *Mycetophylli reesi, Tissue Cell* **33**, 376–387.

Goreau T. F. (1959) The physiology of skeleton formation in coral I: a method for measuring the rate of calcium deposition under different light conditions. *Biol. Bull.* **116**, 59–75.

Goreau T. J. (1977) Coral skeletal chemistry physiological and environmental regulation of stable isotope and trace metals in *Monstastrea annularis*. *Proc. Roy. Soc. Lond. B* **196**, 291–315.

Grassmann O., Neder R. B., Putnis A. and Löbmann P. (2003) Biomimetic control of crystal assembly by growth in an organic hydrogel network. *Amer. Min.* **88**, 647–652.

Grossman E. L. and Ku T. L. (1986) Oxygen and carbon isotope fractionation in biogenic aragonite: temperature effects. *Chem. Geol.* **59**, 59–74.

Grottoli A. G. (2002) Effect of light anf brine shrimp on skeletal $\delta^{13}C$ in Hawaiian coral *Porites compressa*: a tank experiment. *Geochim. Cosmochim. Acta* **66**, 1955–1967.

Grottoli A. G., Rodriges L. J., Matthews K. A., Palardy J. E. and Gibb O. T. (2005) Pre-treatment effects on coral skeletal $\delta^{13}C$ and $\delta^{18}O$. *Chem. Geol.* **221**, 225–242.

Hidaka M. (1991) Fusiform and needle-shaped crystals found on the skeleton of a coral, *Galaxea fascicularis*. In *Mecanism and Physiology of Biomineralization in Biological System* (eds. S. Sugo and H. Nakaharo). Springer, Berlin, Heidelberg, NY, pp. 139–143.

Johnston I. S. (1980) The ultrastructure of skeletogenesis in zooxanthellate corals. *Int. Rev. Cytol.* **67**, 171–214.

Juillet-Leclerc A., Thiria S., Naveau P., Delcroix T., Le Bec N., Blamart D. M. and Corrège T. (2006) SPCZ migration and ENSO events during the 20th century as revealed by climate proxies from a Fiji coral. *Geophys. Res. Lett.* **33**, L17710. doi:10.1029/2006GL025950.

Kim S.-T. and O'Neil J. R. (1997) Equilibrium and nonequilibrium oxygen isotope effects in synthetic carbonates. *Geochim. Cosmochim. Acta* **61**, 3461–3475.

Land L. S., Lang J. C. and Barnes D. J. (1975) Extension rate: a primary control on the isotopic composition of west Indian (Jamaican) scleractinian reef coral skeletons. *Mar. Biol.* **33**, 221–233.

Le Campion-Alsumard T., Golubic S. and Priess K. (1995) Fungi in corals: symbiosis or disease? Interaction between polyps and fungi causes pearl-like skeleton biomineralization. *Mar. Ecol. Prog. Ser.* **117**, 137–147.

Le Tissier M. A. (1988) Diurnal pattern of skeleton formation in *Pocillopora damicornis* (Linnaeus). *Coral Reefs* **7**, 81–88.

Lough J. M. and Barnes D. J. (2000) Environmental control on growth of the massive coral *Porites*. *J. Exp. Mar. Biol. Ecol.* **245**, 225–243.

Lowenstam H. A. and Weiner S. (1989) *On Biomineralization*. Oxford University Press, New York, Oxford, pp. 207–251.

Lutringer A., Blamart D., Frank N. and Labeyrie L. (2005) Deep-sea Coral: a tool to reconstruct changes of intermediate water masses. In *Cold-water Corals and Ecosystems* (eds. A. Freiwald and J. M. Roberts). Springer-Verlag, Berlin, Heidelberg, pp. 1082–1096.

McConnaughey T. A. (1989a) C-13 and O-18 isotopic desequilibrium in biological carbonates: I. Patterns. *Geochim. Cosmochim. Acta* **53**, 151–162.

McConnaughey T. A. (1989b) C-13 and O-18 isotopic disequilibria in biological carbonates: II. In vitro simulation of kinetic isotope effects. *Geochim. Cosmochim. Acta* **53**, 163–171.

McConnaughey T. A. and Whelan J. F. (1997) Calcification generates protons for nutrient and bicarbonate uptake. *Earth Sci. Rev.* **42**, 95–117.

McConnaughey T. A. (2003) Sub-equilibrium oxygen-18 and carbon-13 levels in biological carbonates: carbonate and kinetic modelsM. *Coral Reefs* **22**, 316–327.

McIntyre I. G. and Towe K. M. (1976) Skeletal calcite in living scleractinian corals: microboring fillings, not primary skeletal deposits. *Science* **191**, 701–702.

Mann S., Archibald D. D., Didymus J. M., Douglas T., Heywood B. R., Meldrum F. C. and Reeves N. J. (1993) Crystallization at inorganic organic interfaces: biominerals and biomimetic synthesis. *Science* **261**, 1286–1292.

Marshall A. T. (1996) Calcification in hermatypic and a hermatypic corals. *Science* **271**, 637–639.

Marubini F., Ferrier-Pagès C. and Cuif J.-P. (2003) Suppression of skeletal growth in scleractinian corals by decreasing ambient carbonate–ion concentration: a cross-family comparison. *Proc. R. Soc. Lond.* **270**, 179–184.

Meibom A., Stage M., Wooden J., Constantz B. R., Dunbar R. B., Owen A., Grumet N., Bacon C. R. and Chamberlain C. P. (2003) Monthly strontium/calcium oscillations in symbiotic coral aragonite: biological effects limiting the precision of the paleotemperature proxy. *Geophys. Res. Let.* **30**. doi:10.1029/2002GLO16864.

Meibom A., Cuif J.-P., Hillion F., Constanz B. R., Juillet-Leclerc A., Dauphin Y., Watanabe T. and Dunbar R. B. (2004) Strong biological control over the distribution of magnesium in coral skeleton. *Geophys. Res. Let.* **31**, L23306. doi:10.1029/2004GL021313.

Meibom A., Yurimoto H., Cuif J.-P., Domart-Coulon I., Houlbrèque F., Constantz B., Dauphin Y., Tambutté É., Tambutté S., Allemand D., Wooden J. and Dunbar R. (2006) Vital effect in coral skeletal composition display strict three-dimensional controlM. *Geophys. Res. Lett.* **30**. doi:10.1029/2002GLO16864.

Meibom A., Mostefaoui S., Cuif J.-P., Dauphin Y., Houlbrèque F., Dunbar R. and Constantz B. (2007) Biological forcing controls the chemistry of reef-building coral skeleton. *Geophys. Res. Lett.* **34**, L02601. doi:10.1029/2006GL028657.

Meibom A., Cuif J.-P., Houlbreque F., Mostefanoui S., Dauphin Y., Meibom K. L. and Dunbar R. (2008) Compositional variations at ultra-structure length scales in coral skeleton. *Geochim Cosmochim Acta* **72**, 1555–1569.

Moya A., Tambutté S., Tambutté É., Zoccola D., Caminiti N. and Allemand D. (2006) Study of calcification during a daily cycle of the coral *Stylophora pistillata*: implications for 'light-enhanced calcification'. *J. Exp. Biol.* **209**, 3413–3419.

Muscatine L., Goiran C., Land L., Jaubert J., Cuif J. P. and Allemand D. (2005) Stable isotopes $\delta^{13}C$ and $\delta^{15}N$) of organic matrix from coral skeleton. *Proc. Natl. Acad. Sci. USA* **102**, 1525–1530.

Nothdurft L. D., Webb G. E., Bostrom T. and Rintoul L. (2007a) Calcite-filled borings in the most recently deposited skeleton in live-collected Porites (Scleractinia): implications for trace elements archives. *Geochim. Cosmochim. Acta* **71**, 5423–5438.

Nothdurft L. D. and Webb G. E. (2007b) Microstructure of common reef-building coral genera *Acropora*, *Pocillopora*, *Goniastrea*, and *Porites*: constraints on spatial resolution in geochemical sampling. *Facies* **53**, 1–26.

Ogilvie M. (1896) Microscopic and systematic study of madreporarian types of corals. *R. Soc. Lond. Phil. Trans.* **187**(B), 83–345.

O'Neil J. R., Clayton R. N. and Mayeda T. K. (1969) Oxygen isotope fractionation in divalent metal carbonates. *J. Chem. Phys.* **51**, 5547–5558.

Orme C. A., Noy A., Wierzbicki A., McBride M. T., Grantham M., Teng H. H., Dove P. M. and DeYoreo J. J. (2001) Formation of chiral morphology through selective binding of amino acids to calcite surface steps. *Nature* **411**, 775–779.

Paquette J. and Reeder R. J. (1995) Relationship between surface structure, growth mechanism, and trace element incorporation in calcite. *Geochim. Cosmochim. Acta* **59**, 735–749.

Patterson W. P., Smith, G. R. and Lohmann K. C. (1993) Continental Paleothermometry and seasonality using the isotopic composition of aragonitic otoliths of freshwater fishes. In *Climate Change in Continental Isotopic Records* (ed. P. K. Swart et al.), *Geophys. Monogr. Ser.* **78**, 191–202.

Puverel S., Tambutté É., Pereira-Mouries L., Zoccola D., Allemand D. and Tambutté S. (2005) Soluble organic matrix of two Scleractinian corals: partial and comparative analysis. *Comp. Biochem. Physiol. B* **141**, 480–487.

Raz-Bahat M., Erez J. and Rinkevich B. (2006) In vivo light-microscopic documentation for primary calcification processes in the hermatypic coral *Stylophora pistillata*. *Cell Tissue Res*, doi:10.1007/s00441-006-0182-8.

Reeder R. J. and Hochella M. F. Jr. (1991) Atomic force microscopy of calcite growth surfaces. *GSA Ann. Mfg.,* A216 (abstr.).

Reynaud-Vaganay S., Gattuso J.-P., Cuif J.-P., Jaubert J. and Juillet-Leclerc A. (1999) A novel culture technique for scleractinian corals: application to investigate changes in skeletal $\delta^{18}O$ as a function of temperature. *Mar. Ecol. Progr. Ser.* **180**, 121–130.

Reynaud-Vaganay S., Juillet-Leclerc A., Gattuso J.-P. and Jaubert J. (2001) Effect of light on skeletal $\delta^{13}C$ and $\delta^{18}O$ and interaction with photosynthesis, respiration and calcification in two zooxanthellate scleractinian corals. *Paleogeol. Paleoclim. Paleoecol.* **175**, 393–404.

Rollion-Bard C., Chaussidon M. and France-Lanord C. (2003a) PH control on oxygen isotopic composition of symbiotic corals. *Earth Planet. Sci. Lett* **215**, 265–273.

Rollion-Bard C., Blamart D., Cuif J.-P. and Juillet-Leclerc A. (2003b) Microanalysis of C and O isotopes of azooxanthellate and zooxanthellate corals by ion microprobe. *Coral Reefs* **22**, 405–415.

Rollion-Bard C., Mangin D. and Champenois M. (2007) Development and application of oxygen and carbon isotopic measurements of biogenic carbonates by ion microprobe. *Geostand. Geoanal. Res.* **31**, 39–50.

Sinclair D. J. (2005) Correlated trace element 'vital effects' in tropical corals: A new tool for probing biomineralization chemistry. *Geochim. Cosmochim. Acta* **69**, 3265–3284.

Shin D. W., Ma J. J. and Kim D. H. (2000) The asp-rich region at the carboxyl-terminus of calsequestrin binds to Ca^{2+} and interacts with triadin. *FEBS Lett.* **486**, 178–182.

Shirai K., Kawashima T., Sowa K., Watanabe T., Nakamori T., Takahata N., Amakawa H. and Sano Y. (2008) Minor and trace element incorporation into branching coral *Acropora nobilis* skeleton. *Geochim. Cosmochim. Acta* **72**, 5386–5400.

Smith J. E., Risk M. J., Schwarcz H. P. and McConnaughey T. M. (1997) Rapid climate change in the North Atlantic during the Younger Dryas recorded by deep-corals. *Nature* **386**, 818–820.

Smith J. E., Schwarcz H. P., Risk M. J., McConnaughey T. A. and Keller N. (2000) Paleotemperatures from deep-sea corals: overcoming "vital effects". *Palios* **15**, 25–32.

Swart P. K., Leder J. J., Szmant A. and Dodge R. E. (1996) The origins of variations in the isotopic record of scleractinian corals II. Carbon. *Geochim. Cosmochim. Acta* **60**, 2871–2886.

Tambutté É., Allemand D., Bourge I., Gattuso J.-P. and Jaubert J. (1995) An improved ^{45}Ca protocol for investigating physiological mechanisms in coral calcification. *Mar. Biol.* **122**, 453–459.

Tambutté É., Allemand D., Muller E. and Jaubert J. (1996) A compartimental approach to the mechanism of calcification in hermatypic corals. *J. Exp. Biol.* **199**, 1029–1041.

Tambutté É., Allemand D., Zoccola D., Meibom A., Lotto S., Caminiti N. and Tambutté S. (2007a) Observations of the tissue-skeleton interface in the Scleractinian coral *Stylophora pistillata*. *Coral Reefs* **26**, 517–529.

Tambutté S., Tambutté É., Zoccola D. and Allemand D. (2007b) Organic matrix and biomineralization of scleractinian corals. In *Handbook of Biomineralization* (ed. Edmun Bäuerlein). Wiley-VCH Verlag GmbH & Co., KgaA.

Tarutani T., Clayton R. N. and Mayeda T. K. (1969) The effect of polymorphism and magnesium substitution on oxygen isotope fractionation between calcium carbonate and water. *Geochim. Cosmochim. Acta* **33**, 987–996.

Teng H. H., Dove P. M., Orme C. A. and De Yoreo J. J. (1998) Thermodynamics of calcite growth: baseline for understanding biomineral formation. *Science* **282**, 724–727.

Teng H. H., Dove P. M. and DeYoreo J. J. (1999) Reversed calcite morphologies induced by microscopic growth kinetics: insight into biomineralization. *Geochim. Cosmochim. Acta* **33**, 987–996.

Urey H. C., Lowenstam H. A., Epstein S. and McKinney C. R. (1951) Measurements of paleotemperatures and temperatures of the Upper Cretaceous of England, Denmark, and the southern United States. *Bull. Geol. Soc. Amer.* **62**, 399–416.

Veis A. (2003) Biology in organic matrix framework. In *Reviews in Mineralogy and Geochemistry Volume 54 "Biomineralization"* (eds. P. M. Dove, J. J. DeYoreo and S. Weiner). Mineralogical Society of America, pp. 229–249.

Wainwright S. A. (1963) Skeletal organization in the coral, *Pocillopora damicornis*. *Q.J. Microsc. Sci.* **104**, 169–183.

Weber J. N. and Woodhead P. M. J. (1972) Temperature dependence of Oxygen-18 concentration in reef coral carbonates. *J. Geophys. Res.* **77**, 463–473.

Weirzbicki A., Sikes C. S., Madura J. D. and Drake B. (1994) Atomic force microscopy and molecular modeling of protein and peptide binding to calcite. *Calcif. Tissue Int.* **54**, 133–141.

Wellington G. M., Dunbar R. B. and Merlen G. (1996) Calibration of stable oxygen isotope signatures in Galapagos corals. *Paleoceanography* **11**, 467–480.

Weiner S. and Dove P. M. (2003) An overview of biomineralization. Process and the problem of the vital effect. In *Reviews in Mineralogy and Geochemistry Volume 54 "Biomineralization"* (eds. P. M. Dove, J. J. De Yoreo and S. Weiner). Mineralogical Society of America, pp. 1–29.

Young S. D., O'Connor J. D. and Muscatine L. (1971) Organic material from scleractinian coral skeletons. II. Incorporation of ^{14}C into protein, chitin and lipid. *Comp. Biochem. Physiol.* **40B**, 945–958.

Zeebe, R. E. and Wolf-Gladrow, D. (eds.) (2001) *CO2 in seawater: Equilibrium, Kinetics, Isotopes, 65*. Elsevier Oceanogr, Amsterdam, p. 346.

Zoccola D., Tambutte E., Kulhanek E., Puverel S., Scimeca J.-C. and Allemand D. (2004) Molecular cloning and localization of a PMCA P-type calciumATPase from the coral *Stylophora pistillata*. *Biochim. Biophys. Acta* **1663**, 117–126.

Associate editor: Tim Lyons